Azouaou BERKACHE[1], Zehor OUDNI[1], Hamid MEHADDENE[1], Hassane MOHELLEBI[1], Jinyi LEE[2]

Mouloud Mammeri University (1), Algeria
Chosun University (2), Korea

doi:10.15199/48.2019.08.23

Inspection and characterization of random physical property defects by stochastic finite element method

Abstract. *A stochastic finite element method was applied in the case of 2D magneto dynamic equation to study the detection and evaluation of harmful defect in a conductive structure by InSb Hall sensor and Eddy Currents Non Destructive Testing Technique. The defect is considered as a degradation of physical properties of the material. The electrical conductivity is considered as random variable inside the defect area which is generated using Monte-Carlo method. A statistical treatment was used to study the evaluation of inverse problem. Several global parameters are calculated and discussed.*

Streszczenie. *Przedstawiono przetwornik hallotronowy do badań wiroprądowego nieniszczących. Do projektowania przetwornika wykorzystano stochastyczną metode elementów skończonych. Do rozwiązania odwrotnego problemu wykorzystano metode Monte Carlo. Przetwornik bada zmianę konduktywności materiału spowodowaną istnieniem defektu.* ***Badania nieniszczące z wykorzystaniem wiroprądowego przetwornika Hollla i stochastycznej metody elementów skończonych***

Keywords: stochastic finite element method – hall sensor – random variable – Gaussian type function.
Słowa kluczowe: metoda stochastyczna elementów skończonych - czujnik Halla, - zmienna losowa - funkcja typu Gaussa.

Introduction

Non-destructive techniques are used widely in the industry and science in order to control and evaluate the quality of materials without causing damage [1]. The most commonly used NDT methods are ultrasonic testing (UT), radiography (RT) and eddy current testing [2] .

Eddy Current Testing (ECT) is the standard and one of the most extensively used nondestructive technique method of electric conductivity and magnetic permeability related property in conductive materials in order to evaluate them [1,3]. Whose main applications are found especially in the inspection of aircraft and nuclear industries [4,5], power plants and other engineering constructions [6].

Eddy Current sensors can be made to operate in differential [7] and absolute mode [8]. ECT gain interest in of simple, fast and noncontact testing [9].

Stochastic Finite Element Method SFEM is an extension of the classical deterministic approach for the solution of stochastic problems. It has received considerable attention, due to the rapid development of computer simulation, mathematical modeling and scientific computing to predict and understand the behavior of physical engineering and electromagnetic devices [10,11,12].

The Monte Carlo method is powerful, popular and easy to understand and implement, it is often used in the literature as a reference method in order to check the accuracy of other approaches. It has a large field applications such as analyzing complex problems, development of new material, industrial engineering, simulation of physical process and analysis of nonlinear inverse problems [10,13,14].

Various parameters induce change to the properties of the materials over time which is still in operation, not defective. It's why in this work we assume the defect as a lack of material, corrosion, imperfections of fabrication process or aging. To take in account the effect of random physical properties in defects areas by coupling Monte Carlo method with finite elements method which are used for both detection and evaluation by exploiting a statistical treatment. The principle of this algorithm is to return indeed to distribute *t* random conductivities using the law of large numbers and if necessary we repeat the simulation, a comparison with experimental measurements is realized.

Description of the studied structure and the finite element formulation

Let us consider the studied structure shown schematically in figure.1 [15]. We propose to study a conductive plate having a defect by Eddy Currents non-destructive testing, the sensor moves to the x-axis placed parallel to a flat plate and operate in absolute mode supplied by alternative current of amplitude 0.008 A, which was considered for the measurement of the impedance for both excitation and receiving signal (same coil). The defect area uncertainty can be explained by the change in the distribution of the electric conductivity within this region.

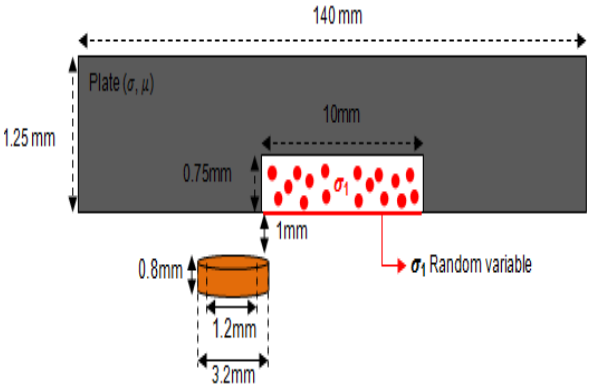

Fig.1.Geometry of the studied problem

The Maxwell equations can be finally derived to 2D electromagnetic equation given in (x,y) coordinates as following [8,15,16]:

$$(1) \quad -\left(\frac{\partial}{\partial x}\left(\nu\frac{\partial A_Z}{\partial x}\right)+\frac{\partial}{\partial y}\left(\nu\frac{\partial A_Z}{\partial y}\right)\right)+j\sigma\omega A_Z = J_{SZ}$$

where: J_{SZ} and A_Z – are the components of current density and magnetic vector along z direction respectively, $\nu = 1/\mu$, μ – the magnetic permeability $[\mathrm{H.m^{-1}}]$, σ and σ_1– are the electrical conductivities $[\Omega.\mathrm{m}]^{-1}$ in the material area and in the defect zone respectively, $\omega=2\pi f$ – the angular frequency, f – represents the frequency of feeding 100 kHz.

With $\sigma_1 = [\sigma_a \ldots\ldots\ldots \sigma_t]$, where t represents the total number of triangles obtained from the mesh in the defect area.

Using the Green theorem and imposing boundary conditions of Dirichlet, type on the boundary of the studied domain, we obtain the following finite elements formulation[8,16] :

$$\iint_{\Omega} \nu \overrightarrow{\nabla \alpha_j} \overrightarrow{\nabla A_z} dxdy + j\omega \iint_{\Omega} \sigma \alpha_j A_z dxdy = \iint_{\Omega} J_{SZ} \alpha_j dxdy \tag{2}$$

$$A_Z(x,y) = \sum_{i=1}^{n} \alpha_i(x,y) A_i \tag{3}$$

where: α_j – projection function, α_i – shape function associated with the node i.

After discritization and assembly we obtain the following complex algebraic system [8,15]:

$$([M] + j\omega[K])[A] = [F] \tag{4}$$

$$M_{ij} = \iint_{\Omega} \nu \vec{\nabla} \alpha_i \vec{\nabla} \alpha_j dxdy \tag{5}$$

$$K_{ij} = \iint_{\Omega} \sigma \alpha_i \alpha_j dxdy \tag{6}$$

$$F_i = \iint_{\Omega} \alpha_i J_S dxdy \tag{7}$$

where: [M] – stiffness matrix, [N] – dynamic matrix, [A] – unknowns vector, [F] – source vector.

Global parameters

In the first part we dealt with the direct problem concerning the development of a mathematical model linking the physical and geometrical characteristics of the studied device. The adopted model allowed us to calculate the impedance of the ECT sensor, current and hall sensor output voltage.

The impedance computation Z is derived using a general method based on the evaluation of the magnetic flux [8,15,17]. The results shown in figure (8) are obtained by exploiting the indicated equations below (8) and (9).

$$\mathrm{Re}(z) = -\frac{N^2}{JS^2} \omega \iint_{S} 2\pi r \,\mathrm{Im}(A) ds \tag{8}$$

$$\mathrm{Im}(z) = -\frac{N^2}{JS^2} \omega \iint_{S} 2\pi r \,\mathrm{Re}(A) ds \tag{9}$$

where: Re(z) and Im(z) – are the real and imaginary parts of the coil impedance respectively, N – coil numbers, S – surface coil, r – inductor radius.

The induced current in the defect zone is given by the relation below:

$$I = \iint_{\Omega} -j\sigma\omega A dxdy \tag{10}$$

The magnetic field produced by eddy currents around the defect is distorted and it can be measured by hall sensor [9,18]:

$$V_H = I_H(K) B_z \tag{11}$$

$$V_{RMS} = \sqrt{\frac{1}{T} \int_0^T V_H(t) dt} \tag{12}$$

where: V_H – Hall sensor output voltage, I_H – sensor input current , k – sensor coefficient constant, B_z – magnetic flux density along z direction, V_{RMS} – root mean square voltage.

Simulation results

The mesh of the domain corresponding to the studied structure is given in figure 2.

Figure.3. show the random distribution of the electrical conductivity inside the defect zone.

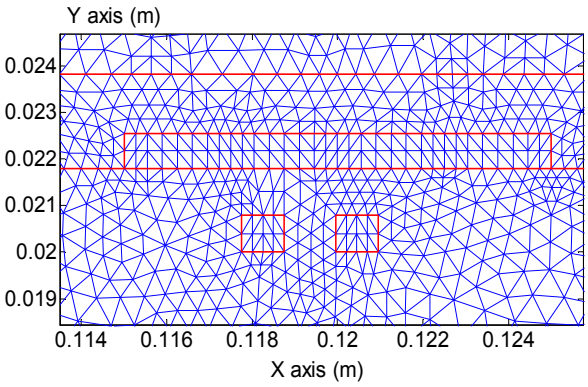

Fig.2. The mesh of defect area and coil

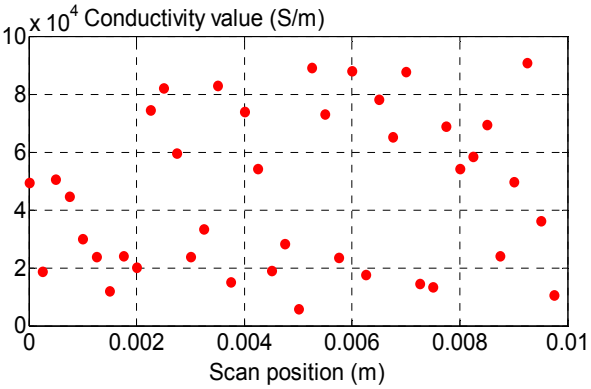

Fig.3. The electrical conductivity distribution along the defect area

The law of probability that we have used for in this work, as expressed by the relation (13), allows us to describe in a theoretical way the random character of the experiment that we have modeled. The study of the stochastic nature of the physical property let us to consider several distributions of this property. This induces a trivial interest in the physical behavior of the electrical conductivity in the defect area. The probability density of electrical conductivity values occurring is considered random and of normal distribution given by [15,19]:

$$f(x) = \frac{1}{S\sqrt{2\pi}} e^{-\frac{1}{2}\left(\frac{x-E}{S}\right)} \tag{13}$$

With: x – the random variable, E – the expectation, S – the standard deviation.

The obtained distribution has the same behavior than one encountered in theory as a standard evolution.

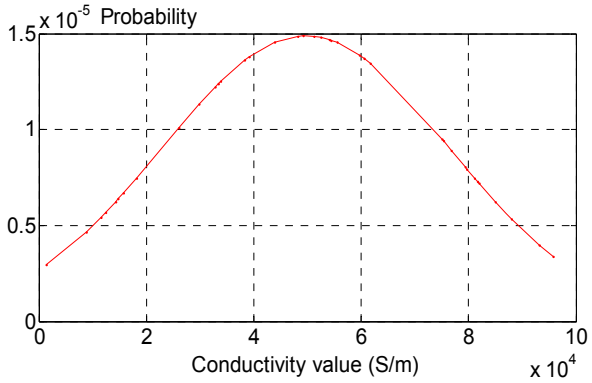

Fig.4. Probability density of the electrical conductivity obtained with one print

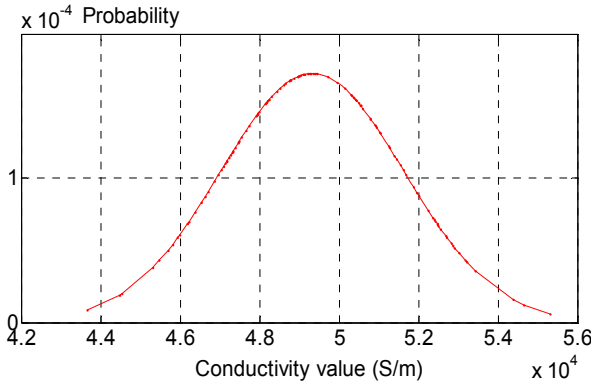

Fig.5. Probability density of the mean of the electrical conductivities

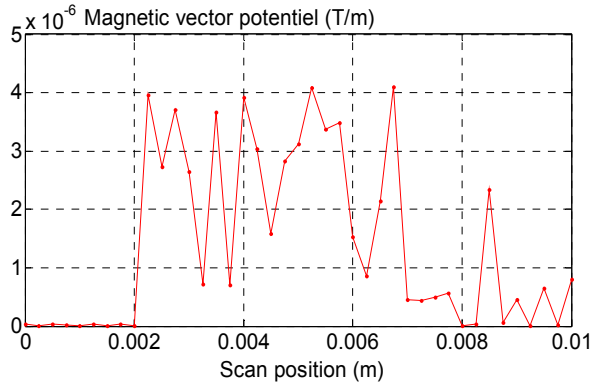

Fig.6. The magnetic vector potential in the defect area

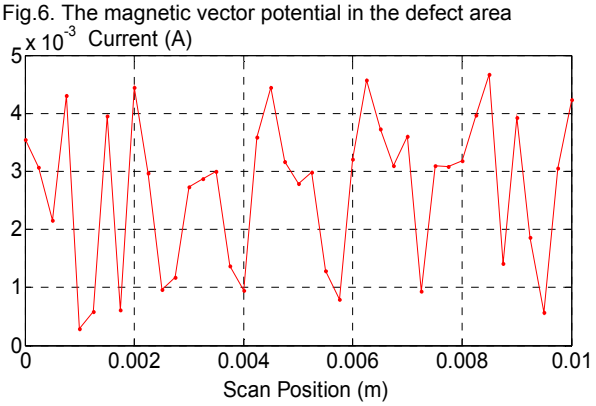

Fig.7. The current variation for different position in the defect area

The total current in the defect zone decreases in amplitude comparing to the injected one.

The amplitude fluctuations obtained in deterministic case are insignificant or negligible. In contrast it changes in the defect area due to the presence of the defect.

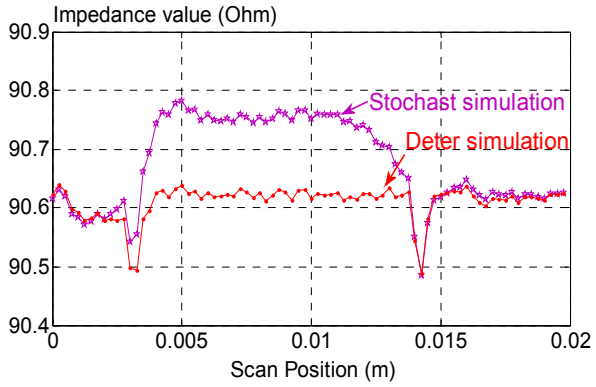

Fig.8. The impedance variation according to scan position

Experimental setup

In our experimental setup two types of defects are investigated: crack and degradation. The second one is considered as an impurity and in order to show the effect of uncertainty we used a defects of dimensions adapted to the experiment carried out given in table 1. Three different experiments are performed .

Experiment (1)

The first experiment consist on GW-INSTEK 8101G LCR- meter which produces the excitation voltage, a pancake coil and conductive plate (with and without defect)

This experiment is characterized by the parameters given in table 1. The impedance signal obtained from the ECT probe is recovered and represented as a function of the sensor's position. A comparison with the simulation work is done.

Table 1. Parameters of the test experiments

Coil	Plate	Defect
Inner diameter 10 mm	Thickness 2 mm	A/- Crack Length 10 mm Width 2 mm Depth 1 mm
Outer diameter 12 mm	Electric conductivity 58 MS/m	
Height 6 mm	Relative permeability 1	B/- Degradation Length 10 mm Width 2 mm Depth 0.5 mm
Number of turns 200	Lift-off 1 mm	

Experiment (2)

The second experimental setup one is realized by using LabVIEW software program to generate the real time application and to monitor the output signal. The variation of the output voltage is calculated, analyzed and stored according to the position of the Hall sensor. Exciting coil: 310 turns – inner diameter 7.45 mm – outer diameter 9.7 mm height 4 mm and scan speed 10 mm/s.

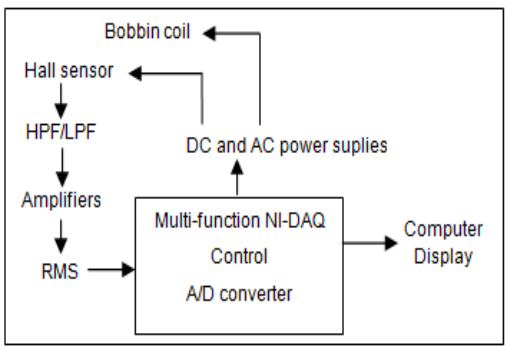

Fig.9. Scheme of the second experimental setup

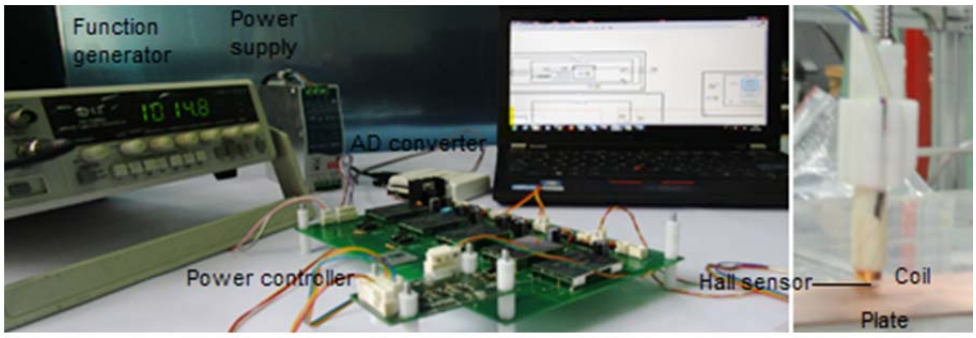

Fig.10. Photograph of the second experimental setup

The scan was done on the x-y plan of the defect area with a frequency of 1kHz and 10 kHz respectively. The schematic and the photograph of the experiment setup is shown in figures. 9 and 10. The signal output of the Hall sensor (V_H) is processed through high-pass filters/law-pass filters (HPF/LPF), amplifiers, root-mean-square circuits (RMS,V_{RMS}) , A/D converter and displayed in a computer.

Experiment (3)

The third experimental is realized by Nortek 500 portable eddy current flaw detectors, a probe with range of frequency 100 kHz to 500 kHz in absolute mode is used.

Experimental results and discussion

The results presented below in figure 11 concerns the validation of the experiment results related to the studied NDT structure obtained with ECT probe. They are compared to the numerical one obtained using stochastic finite element method developed under Matlab software given in relative values.

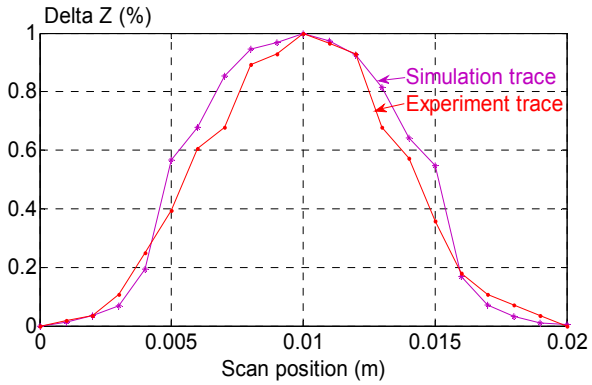

Fig.11. Numerical computed impedance vs experimental one according to scan position in relative value at 100 kHz

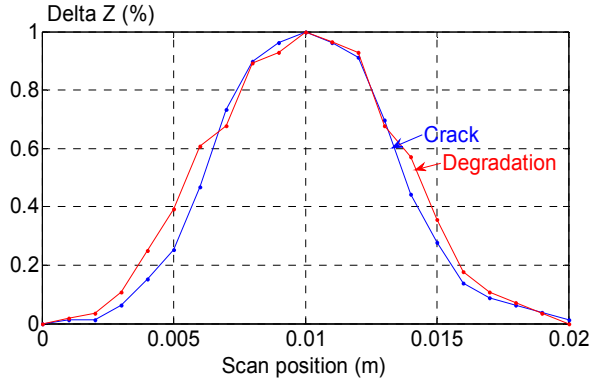

Fig.12. The impedance variation according to scan position in relative value obtained by experiment at 100 kHz

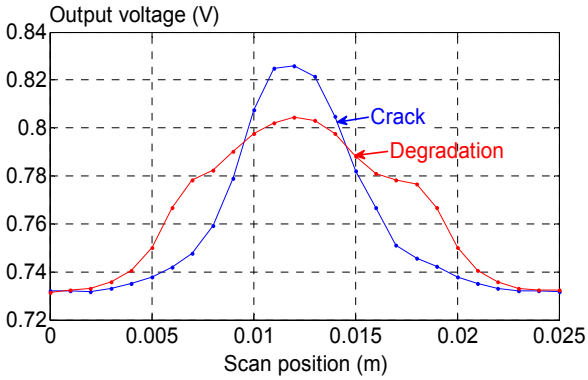

Fig.13. Hall sensor output voltage according to scan position on the width of the defect obtained by experiment at 10 kHz

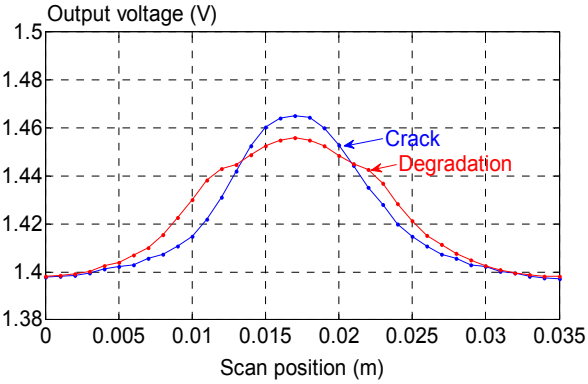

Fig.14. Hall sensor output voltage according to scan position on the length of the defect obtained by experiment at 1 kHz

The figures 12,13 and 14 show a comparison of the shape of the defect to distinguish the nature of anomalies obtained by experiment with ECT probe and Hall sensor respectively. Third experimental setup is realized by Nortek 500 portable.

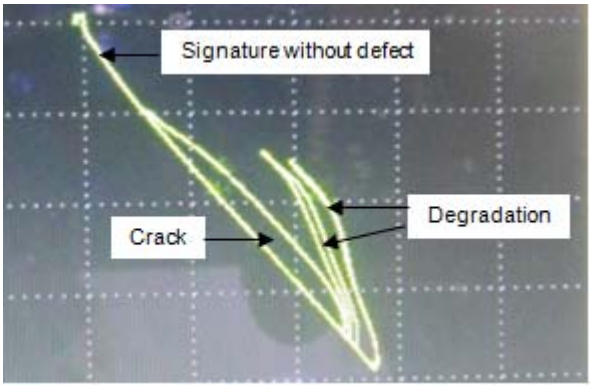

Fig.15. The Impedance plan.

Figure 15 gives the signature of the material in presence or absence of the anomalies on the impedance plan.

Evaluation

The idea behind this section, is to exploit a statistical treatment, the data from the simulation are used to estimate the size of the defect, which we are looking for in the current application relying on the analyze of probabilistic data such as variance, mean and standard deviation of the impedance computation given below [19].

The dimensions of the simulated samples are given in table 2.

$$E(x) = \sum_{i=1}^{t} x_i p_i \tag{14}$$

$$V(x) = \frac{1}{t} \sum_{i=1}^{t} p_i (x_i - m) \tag{15}$$

$$S = \sqrt{V(x)} \tag{16}$$

With: x_i – the random variable, p_i – probability of x_i, E – the expectation, V – the variance, S – the standard deviation

Table 2. The different dimensions of the simulated samples

Defect dimensions	Width [mm]	Length [mm]
defect 1	1.25	140
defect 2	1	88.5
defect 3	0.75	10

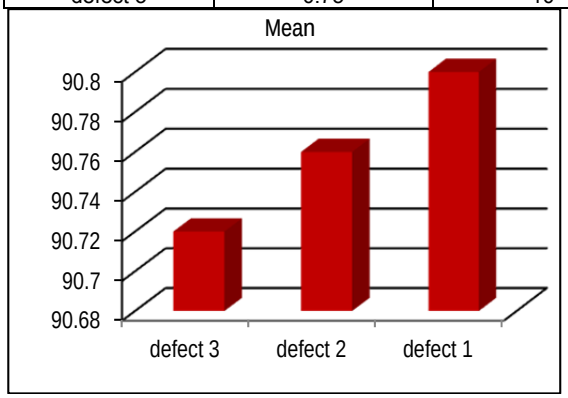

Fig.16. Correlation between the mean of the impedance values and the defects size.

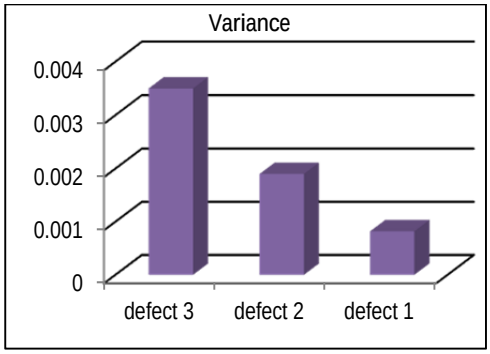

Fig.17. Correlation between the variance of the mean of the impedance values and the defects size

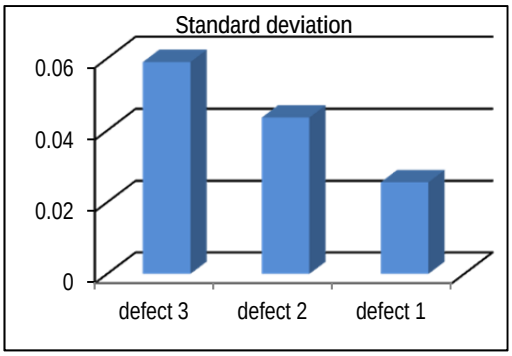

Fig.18. Correlation between standard deviation of the mean of the impedance values and the defects size.

The dispersion of the standard deviation and the variance obtained (retrieved) from the distribution in relation to the average (mean) is low. The values are not very far apart, that means there are a lot of impedance values since they are very close. This implies that the defect is important which corresponds to the defect1. But for the defect3, the values of the statistical quantities are more important than the two others cases. That implies there are few impedances values, consequently we recover the following information that the defect is small and corresponds to the case shown in the fig.1. In the case of a punctual defect (too small defect), the values are nulls, consequently there is no variation of the statistical variables.

A summary scheme of resolution is presented in figure (19) given below.

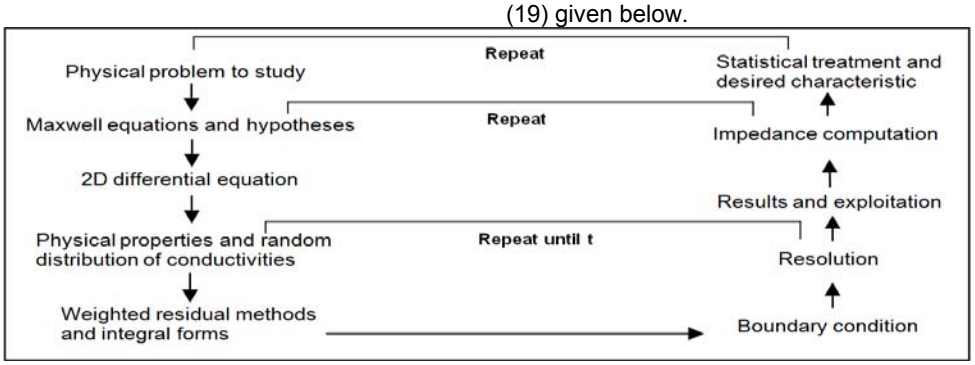

Fig.19. Synthesis flowchart under Matlab

Conclusion

This paper presents the efficient application of SFEM for detection and evaluation of defect area uncertainty. Monte Carlo simulation was exploited to generate the electrical conductivity as random variable which is the main parameter of this study applied for NDT problem. In this case the average of all those distributions is represented as probability density function which has the same behavior as it is given in theory.

The first part of this work concerns a detection of the defect and then a comparison with the deterministic case

is made. The results are that from both impedance and hall sensor voltage the nature of the anomaly is being visible. The second one is dedicated to the evaluation of defect sizes with probabilistic. But the computational time is little expensive.

The measurement results concerning the validation of the experimental data of the studied structure obtained by LCR- meter are in good agreement with numerical results.

***Authors**: PhD student. Azouaou Berkache, Numerical Modeling of Electromagnetic Phenomena and Components Laboratory, Mouloud Mammeri University of Tizi-Ouzou, BP 17RP 15000, Algeria, E-mail: azouaoubrk@yahoo.fr; dr. Zehor Oudni, Numerical Modeling of Electromagnetic Phenomena and Components Laboratory, Mouloud Mammeri University of Tizi-Ouzou, BP 17RP 15000, ALGERIA, E-mail: z_oudni@yahoo.fr; PhD student. Hamid Mehaddene, Numerical Modeling of Electromagnetic Phenomena and Components Laboratory, Mouloud Mammeri University of Tizi-Ouzou, BP 17RP 15000, Algeria, E-mail: mehaddenehamid@yahoo.com.; prof. dr. Hassane Mohellebi, Numerical Modeling of Electromagnetic Phenomena and Components Laboratory, Mouloud Mammeri University of Tizi-Ouzou, BP 17RP 15000, ALGERIA, E-mail: mohellebi@yahoo.fr; prof. dr. Jinyi Lee, Research centre for Real Time NDT, Chosun University , 375, Seosuk-dong, Gwangju, 61452, Korea, E-mail: jinyilee@chosun.ac.kr*

REFERENCES

[1] Rifai D., Abdalla A.N., Ali K., Razali R., Giant Magnetoresistance: A review on Strucures and Non Destructive Eddy Current Testing Applications, *Sensors (Switzerland)*., 16 (2016), No.3, doi: 10.3390/s16030298.

[2] Rosado L.S., Santos T.G., Piedade M., Ramos P.M., Vilaça P., Advanced Technique for Non-Destructive Testing of Friction Stir Welding of Metals, *Meas.J.Int.Meas.confed*., 43 (2010), No.8, 1021-1030

[3] Gäbler S., Heur H., Heinrich G., Measuring and Imaging Permittivity of Insulators Using High-Frequency Eddy-Current Devices, *IEEE Trans. Instum.Meas*., 64 (2015), No. 8, 2227-2238

[4] Teagle P.R., The Quality Control and Non-Destructive Evaluation of Composite Aerospace Components, *Composite*., 14 (1983), No. 2, 115-128

[5] Förster F., Sensitive Eddy-Current Testing of Tubes for defects on the Inner and Outer surfaces., *Non-Destructive Test*., 7 (1974), No.1, 28-36

[6] Morozov M., Rubinacci G., Tamburrino A., Ventre S., Numerical Models of Volumetric Insulating Cracks in Eddy-Current Testing With Experimental Validation, *IEEE Trans. Magn*., 42 (2006), No.5, 1568-1576

[7] Hamel A., Mohellebi H., Féliachi M., Imperialist Competitive Algorithm and Particle Swarm Optimization Comparison for Eddy Current Non-destructive Evaluation, *Przegląd Elektrotechniczny* (Electrical Review), R. 88 NR 9a/2012, ISSN 0033-2097.

[8] Mehaddene H., Mohellebi H., Berkache A., Eddy Currents Non Destructive Testing and Evaluation of Ferromagnetic Medium, *Przegląd Elektrotechniczny*, R. 95 NR 2/2019 ISSN 0033-2097, 112-116

[9] Lee J., Hwang J., Jun J., Choi S., Nondestructive Testing and Crack Evaluation of Ferromagnetic Material by Using Integrated Hall Sensor Array, *J. Mech. Sci. Technol*, 22 (2008), No.12, 2310-2317

[10] Stefano G., The Stochastic Finite Element Method: Past,Present and future, *Comput. Methods Appl. Mech*, 198 (2009), No.9-12, 1031-1051

[11] Enokizono M., Aoki M., Application of Stochastic Finite Element Method to the Analysis of Magnetic Field, *IEEE Trans. J. Magn.Jpn,* No.2 (1987), 973-981

[12] Beddek K., Clénet S., Moreau O., Costan V., LeMenach Y., Benabou A., Adaptive Method for Non-Intrusive Spectral Projection Application on a Stochastic Eddy Current NDT problem, *IEEE Trans. Magn*.,48 (2012), No.2, 759-762

[13] Beddek K., Clénet S., Moreau O., LeMenach Y., Solution of Large Stochastic Finite Element Problems—Application to ECT-NDT, *IEEE Trans. Magn*., 49 (2013), No.5, 1605-1608 Pike G.E., Preparation of Papers for Transactions, *IEEE Trans. Magn*., 50 (2002), No. 5, 133-137

[14] Moseggard K., Sambridge M., Monte Carlo Analysis of Inverse Problems, *Institute of Physics Publishing*, 18 (2002), 29-54

[15] Oudni Z ., Feliachi M., Mohellebi H., Assessment of the Probability of Failure for EC Nondestructive Testing Based on Intrusive Spectral Stochastic Finite Element Method, *Eur. Phys. J. Appl. Phys*, 66 (2014), No.5, 133-137

[16] Ayad A., Benhamida F., Bendaoud A., Le Bihan Y., Bensetti M., Solution of Inverse Problems in Electromagnetic NDT Using Neural Networks, *Przegląd Elektrotechniczny* (Electrical Review), R. 87 NR 9a(2011), ISSN 0033-2097

[17] Thomas J-L., Simplified Modeling of Eddy Current Control of Steam Generator Tubes Report of internship ESA IGELEC, 1998, University of Nantes, France

[18] Kim J., Le M., Lee J., Hwang Y.H., Eddy current Testing and Evaluation of Far-Side Corrosion Around Rivet in Jet-Engine of Aging Supersonic Aircraft, *J. Nondestruct. Eval*, 33 (2014), No.4, 471-480

[19] Loeve M., Probability Theory I, forth edition, *Springer-Verlag Inc*, 45 (1977), DOI 10.1007/978-1-4684-9464-8